DESIGN AND EXPERIMENTAL INVESTIGATION OF TRANSONIC NATURAL LAMINAR FLOW WINGS

J. Hua, Q.Z. Yang, D.K. Xi, Z.Y. Zhang
Northwestern Polytechnical University (NPU), China
D.W. Fu
Xi'an Aircraft Company (XAC), China
Z.L. Zhang, L. Wang
Nanjing University of Aeronautics and Astronautics(NUAA),China

Abstract

Flow laminarization has been clearly regarded as the technique for the next generation of transport aircraft, but suitable design methods are still under investigation. After the description of a transonic 2D/3D-design method based on the modified "iterative residual correction" principle, design practice of transonic backward swept and forward swept NLF wings and wing-bodies with this method is discussed, including the isobar criterion and the specification of target pressure distributions. The examples show that it is necessary to take viscous and body effects into account in the design methods. Wind tunnel tests on the low and high speed models of a designed NLF wing are conducted. The measurements show stable laminar flows, straight transition lines and clear drag reductions, suggesting that the present numerical methods, design and experimental techniques are practical for developing transonic and NLF configurations.

1. Introduction

Successive worldwide research on flow laminarization in the last decade, mainly for transport wings, has demonstrated a new potential of drag reduction in the order of 15% with respect to the total aircraft drag[1],[2]. This success launched also investigations on laminar flow fins, nacelles and supersonic laminar flow wings[3]. In industry a design practice of a regional jet transport with NLF (Natural Laminar Flow) wing has been once performed[4].

Besides LFC (Laminar Flow Control) and HLFC (Hybrid LFC) techniques, NLF approach by appropriately shaping the wing geometry to keep laminar boundary layer up to 50% or 60% of the wing chord has been assessed to be favourable for wings with moderate cruise Re (Reynolds) number, so it has attracted much attention.

The development of such modern design techniques depends greatly on the progress of CFD (Computational Fluid Dynamics) and new experimental methods. With the help of computer software, flow analysis around complex 3D (3-Dimensional) configurations based on accurate mathematical models like Euler and NS (Navier-Stokes) equations has become possible, which leads to the name of Numerical Wind Tunnels[5]. Codes for 3D-boundary layer stability analysis are also under validation with the data accumulated from special wind tunnel and flight tests[6]. Infrared image, hot film and piezo foil techniques have really supported the measurements[7].

However, recent design practice indicates that only the CFD codes capable of giving results within a few hours or days could actually play the key roles[8]. Then the so called "inverse methods" which generate desired geometries for specified flow fields become even more important. But few efforts have been concentrated in this aspect compared with "direct problems". Of those successful[9-12], the 3D-transonic wing design method of Takanashi[12] based on potential equation is still considered the state of the art. Meanwhile Giles/Drela[13] and Hirose[14] are among the pioneers developing 2D-inverse methods based on Euler and NS equations, respectively.

What still remains open is the problem that most of the existing transonic inverse methods are confined to full turbulent flows or inviscid at all. NLF configurations generated by using such methods often fail to realize the target pressure coefficient (Cp) distributions , if checked under mixed laminar-turbulent flow conditions. Then the configurations would have to be modified repeatedly and the target Cp distribution could seldom be completely reached. This problem forms the background of the present investigation.

In the last few years a Two-Dimensional Three-Dimensional Transonic Design software NPU-TDTDTD has been developed originally for generating supercritical airfoils and wings, and then extended to design NLF configurations[15-19]. Accompanying the development of the 3D-method, several design examples of NLF wings and wing-body combinations, including Forward Swept Wings(FSW), are made. Experimental research on the low and high speed wind tunnel models of the NPU-NLF1 wing, one of the examples, has been carried out in order to check the numerical methods and design criteria. This wing design and experimental research will be discussed in the following chapters.

2. Numerical Methods and Software

Based on the "iterative residual correction" principle of Takanashi[12], the design procedure consists of two modes: inverse and direct steps executed iteratively following the flow-chart shown in Fig. 1:

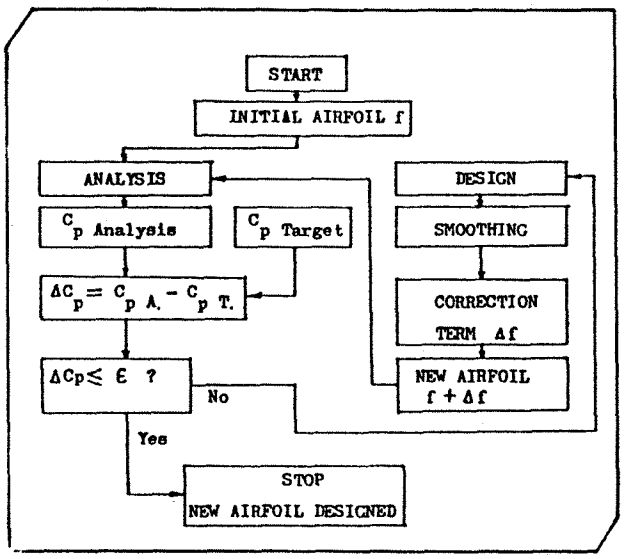

Fig. 1 Flow-chart of the design procedure

2.1 Inverse Methods

The 2D and 3D-inverse methods are developed using the integral formulation initiated from full potential equation with small perturbation assumption to the "residual potential $\Delta\varphi$" as described in[12]. Major modifications such as the following have been proven to be necessary and effective[15-19]:

- The numerical integrations used in[12] have all been replaced by closed form integral representations carefully derived. The removal of different singularities has been the key facts in this process, e.g. in 2D-formulas one integral :

$$\mu'_{ik}=\frac{1}{\pi}[(1-\delta_{k,J+1})I_{ik}+(1-\delta_{k,1})\hat{I}_{ik}] \qquad (1)$$

could be derived as :

$$I_{ik}=\frac{x_i-x_{k+\frac{1}{2}}}{x_{k+\frac{1}{2}}-x_{k-\frac{1}{2}}}\ln\left|\frac{x_i-x_{k+\frac{1}{2}}}{x_i-x_{k-\frac{1}{2}}}\right|+1 \qquad (2)$$

$$\hat{I}_{ik}=\frac{x_{k-\frac{3}{2}}-x_i}{x_{k-\frac{1}{2}}-x_{k-\frac{3}{2}}}\ln\left|\frac{x_i-x_{k-\frac{1}{2}}}{x_i-x_{k-\frac{3}{2}}}\right|-1 \qquad (3)$$

- In order to ensure satisfactory convergence in the supersonic regions and near the shocks, a supersonic adaptive weighting function in the weighted smoothing procedure introduced in[15] is further constructed as:

$$WF(x)=0.3WF_1(x)+0.7WF_2(x) \qquad (4)$$

where

$$WF_1(x)=\{0.5[\cos 2\pi\,(x^{-\frac{\ln 2}{\ln x_{s1}}}-0.5)+1]\}^{P_W} \qquad 0\leqslant x<x_{s1}$$

$$WF_1(x)=1 \qquad x_{s1}\leqslant x\leqslant x_{s2}$$

$$WF_1(x)=\{0.5[\cos 2\pi\,(x^{-\frac{\ln 2}{\ln x_{s2}}}-0.5)+1]\}^{P_W} \qquad x_{s2}<x\leqslant 1$$

$$WF_2(x)=|C_{pT}(x)-C_p^*|/(C_{pT}-C_p^*)_{max} \qquad x_{s1}\leqslant x\leqslant x_{s2}$$

with x_{s1} and x_{s2} being the first and last supersonic points on the airfoil surface.

- Matrix condition analysis implemented offers real-time estimation of the rationality of the mesh distributions.

2.2 Viscous Corrections

One of the most important criteria among those put forward in[16] for the assessment of a practical inverse method is that viscous effect must be taken into account during the design phase, especially for transonic flows and NLF configurations. Even though the original method of Takanashi[12] is inviscid, the principle itself suggested a potential of viscous correction which was then cleared up by Hirose[14], who coupled a 2D-NS code with the 3D-inverse code of Takanashi[12] for airfoil design, and the viscous effect was naturally included in the NS calculations. Put forward in the present method is the approach known as "direct viscous iteration" for those direct codes other than NS but with

boundary layer corrections. In this approach the inverse codes correct only the wing contours while boundary layer calculations and viscous corrections are performed in each of the analysis step. Because the difference of displacement thickness δ^* between each iteration is much smaller than the contour correction terms, the overall convergence of Cp distributions would not be largely affected. The main features are:

- The treatment of adding and subtracting δ^* to and from the designed contours is done automatically in the analysis.
- The direct code could still be treated as a "black-box", so once a new direct code with better ability such as mixed boundary layer corrections for NLF configurations becomes available, design of such configurations could be realized simply by coupling the new code with the inverse one. This approach has been demonstrated successful by a number of 2D and 3D design examples.

2.3. Method for Wing-Body Combinations

The above principle of viscous corrections applys also to other effects like the influence from the fuselage or nacelles. The approach is to couple with the inverse method those direct codes capable of analyzing wing-body combinations, wing-nacelle combinations or even complete aircraft.

2.4. Direct Methods

Coupled with the 2D and 3D-inverse codes, respectively, are several transonic airfoil and wing analysis methods, such as well known BGK, FLO22, FLO27 and some more advanced codes[20-23]. Methods used in this work are FLO-22 and mainly FLO27-vis. The latter is a transonic wing-body analysis code including mixed boundary layer correction[24], in which the attachment line transition (ALT) is estimated by a critical Re number suggested by Cumpsty and Head, transition due to crossflow instability (CFI) is determined by using a critical Re number recommended by Boltz, and streamwise flow transition due to Tollmien- Schlichting instability (TSI) is checked by the existing results corresponding to the Falkner-Skan family of similar velocity profiles transformed from virtual incompressible flow field by Stewartson transformation. The calculation results have been compared with wing test data available.

2.5. NPU-TDTDTD Software

Fig. 2 shows the current status of NPU 2D/3D Transonic Design software, which is used to design supercritical, NLF and conventional airfoils and wings, usually within a few inverse/direct iterations. The high aerodynamic efficiency and smooth curvature of the designed contours demonstrate the performance of this software. The unique feature is that both 2D and 3D-methods are based on the same theory, same program structure and same input formating, with the help of real-time on-screen-display of the design process and results, the software is found to be practical for both 2D and 3D applications. Codes combinations shadowed in Fig. 2 are used in this paper for NLF wing designs.

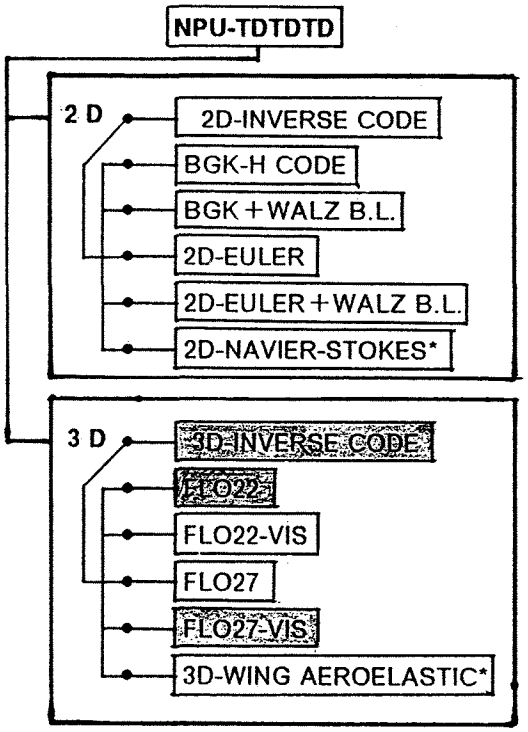

* under way

Fig. 2 Current structure of NPU 2D/3D Transonic Design software

3. Design of NLF Wings

3.1 Design Criteria

Fig. 3 shows a typical Cp distribution of a NLF airfoil for transport aircraft at design condition, in which the leading edge suction peaks, the amount of front loading and the slope of the straight acceleration parts are all carefully specified following the corresponding criteria from the investigation of different laminar flow instabilities[25].

But in 3D case, suitable criteria are still under investigation. Then a straight isobar criterion is suggested and used for transonic NLF wing design in this paper due to the following considerations:

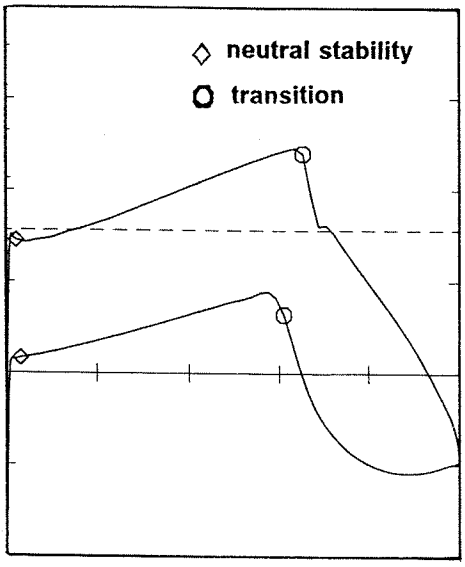

Fig. 3 Typical Cp distribution of a modern NLF airfoil[25]

- It could, in a large span area, retain 2D Cp distributions of the baseline airfoil for which the 2D criteria have been considered.
- Avoiding additional cross flows over the wing surface caused by pressure gradients in the span direction.
- The relative thickness of the outer wing may increase in the span direction which could reduce the induced sweep angle of the wing[26].

3.2 Design of Backward Swept Wings

Design condition of the wing is Mach number M=0.75, lift coefficient Cl=0.5 at Re number 10 million. The aspect ratio is 11 and leading edge sweep angle 19°.

NPU-L72513 airfoil developed at NPU Airfoil Research Center is used as the baseline profile which was designed at M=0.72, Cl=0.5 and relative thickness t/c = 13%[27].

3.2.1 Design of Wing Alone

An initial wing is constructed by putting the baseline airfoil into each of the six control sections along the wing span, say z=0.0, 0.1, 0.3, 0.6, 0.8 and 1.0, where the target Cp distributions are also specified following the isobar criterion as shown in Fig. 4. The upper-side Cp distributions from z=0.1 to 0.8 semispan are the same, while at the tip and root sections the suction level is reduced for thickness control. The lower-side Cp targets at each control section are different in order to have an elliptical load distribution in the span direction.

Design case 1:

In a first design case, inviscid code FLO22 was

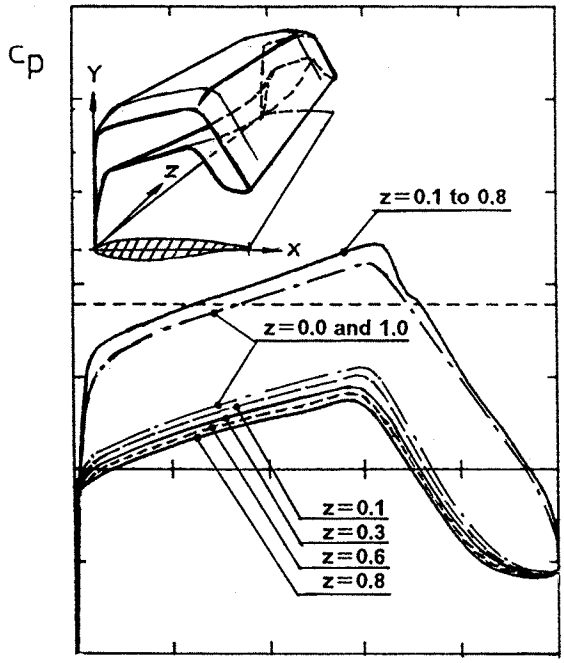

Fig. 4 Target Cp distribution of a NLF wing

used as the direct method so δ^* from a 2D-analysis is added to each control section. 4 design iterations led to a satisfactory convergence as shown in Fig. 5. The transition between 62% to

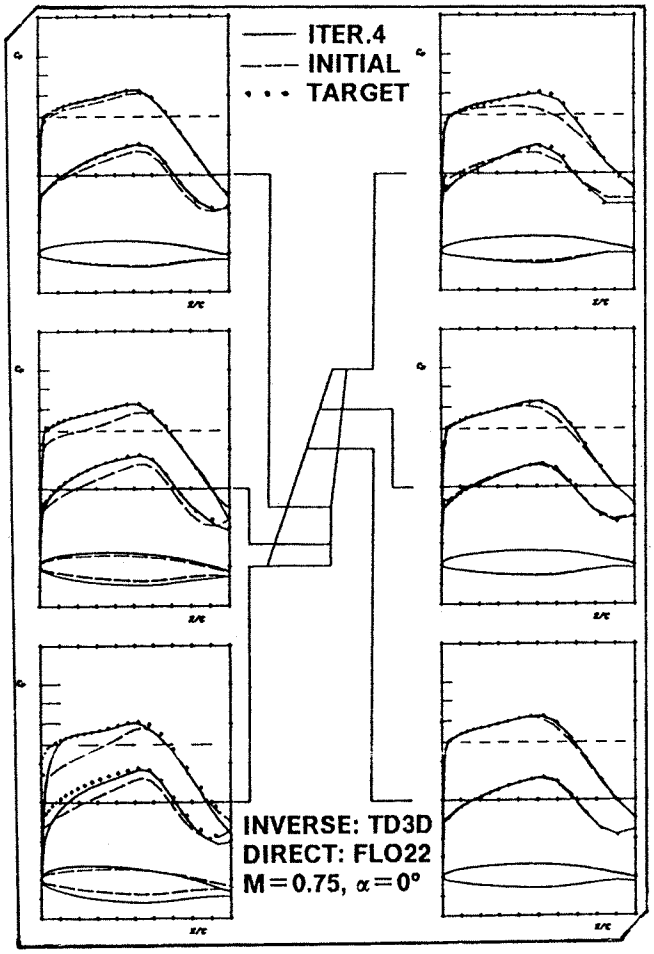

Fig. 5 Design result of NLF1 wing (Case 1)

65% chord on the upper surface around design conditions was estimated with a 3D-boundary layer stability analysis method[28]. This wing was named NPU-NLF1.

Design case 2:

When FLO27-vis code[24] becomes available, this wing was designed again using "direct viscous iteration" approach, so treating δ^* has not been necessary. The target Cp is obtained by the calculation of NLF1 wing under design condition with the new code. The transition behaviour is found close to the stability analysis. The initial wing is made the same way as in Case 1, except that the root section takes directly the one of NLF1 wing and is kept unchanged during the design. After 6 design iterations the Cp distributions and the wing contours are all very well converged to the original NLF1 wing, as shown in Fig. 6.

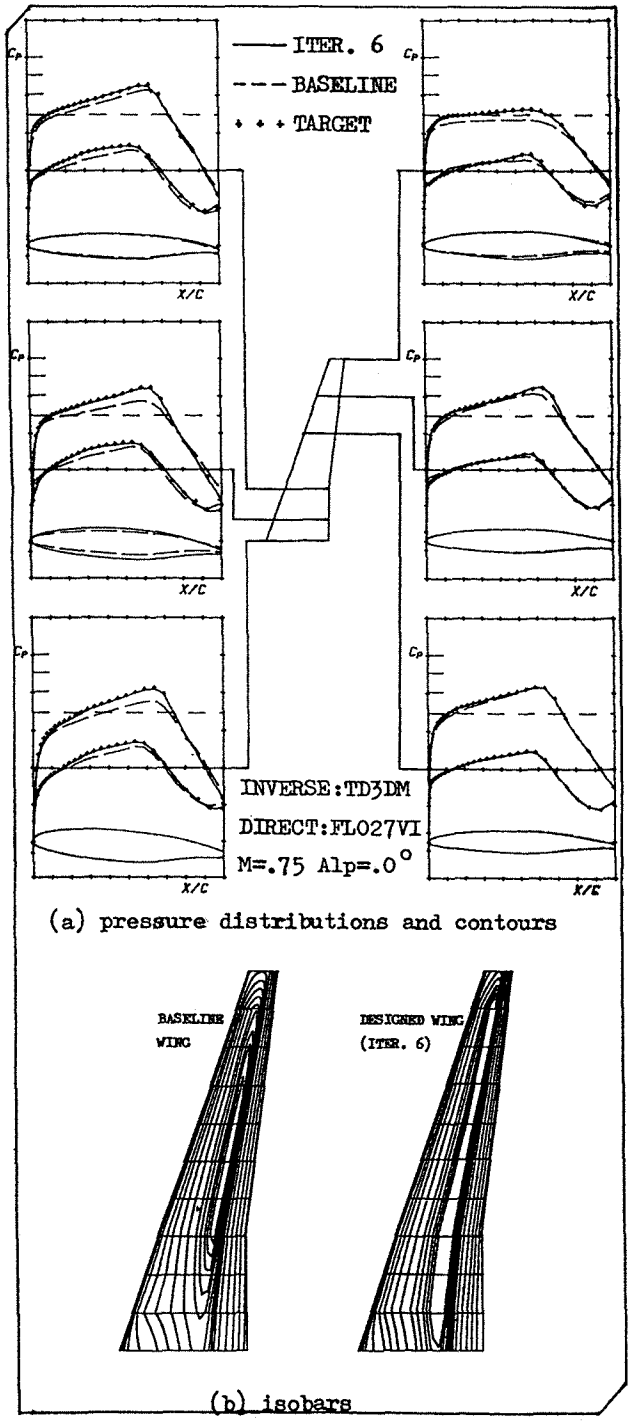

Fig. 6 Design result of NLF1 wing (Case 2)

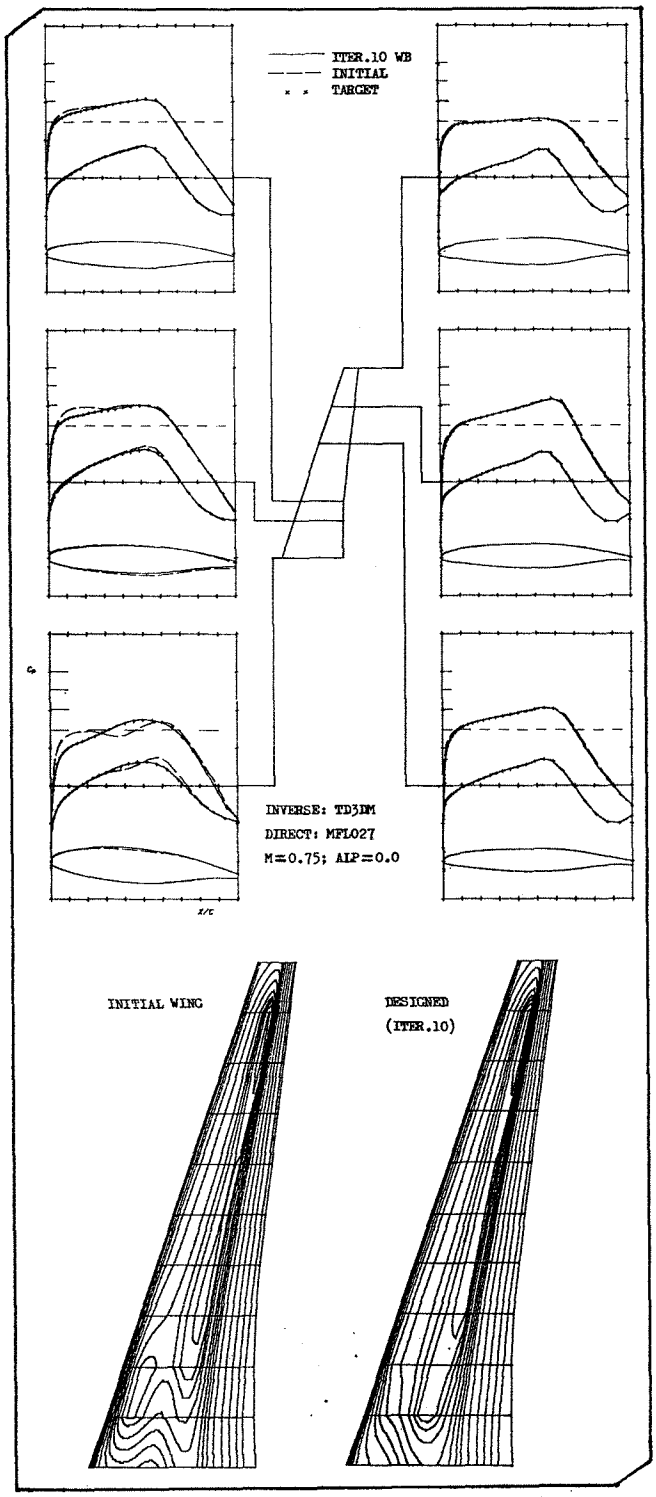

Fig. 7 Design result of NLF1 wing-body

3.2.2 Design of Wing-Body

When the NLF1 wing was calculated again by using FLO27-vis code with bodies of different radii, Cp distributions change greatly, a saddle shape Cp appears at the inboard sections and laminar flow becomes quite unstable.

The design is then repeated again taking body effect into account. After 10 iterations the original Cp target is reached again, as shown in Fig. 7. Fig. 8 shows the difference of control section contours with and without body effects. The root section becomes thicker and the section next to root is getting thiner, in order to retain the same Cp distribution as wing alone.

3.3 Design of Forward Swept Wing

Forward swept wing (FSW) has been shown to be favourable over backward swept wings (BSW) for NLF[26]. So a combined VC(Variable Camber)-NLF-FSW would represent the New Concept Wings for the future transport aircraft, and the investigation should be initiated.

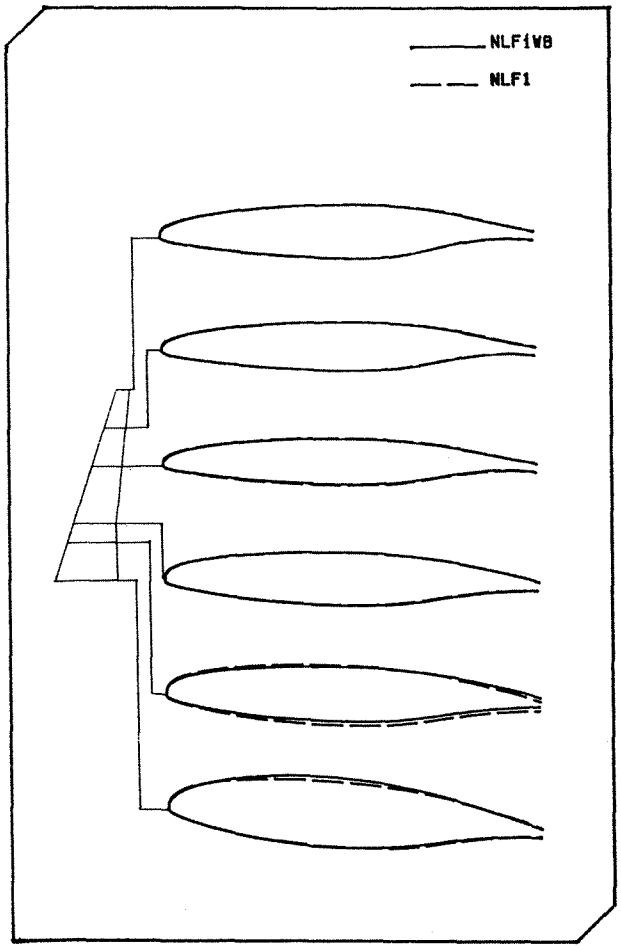

Fig. 8 Comparison of wing control sections with and without body

3.3.1 Design of FSW Alone

The NLF1 wing discussed above is converted into a FSW by changing the quarter chord line sweep angle from 17.2° into −17.2° and the twist adjusted. Analysis shows that the inboard Cp distributions change in the way that strong suction appears near the leading edge (see Fig. 9 noted as INITIAL wing). Then a new inboard Cp distribution is re-specified in this manner that straight isobar could be retained near the wing root area. With the present method, 4 iterations lead to a reasonable convergence, as shown also in Fig. 9.

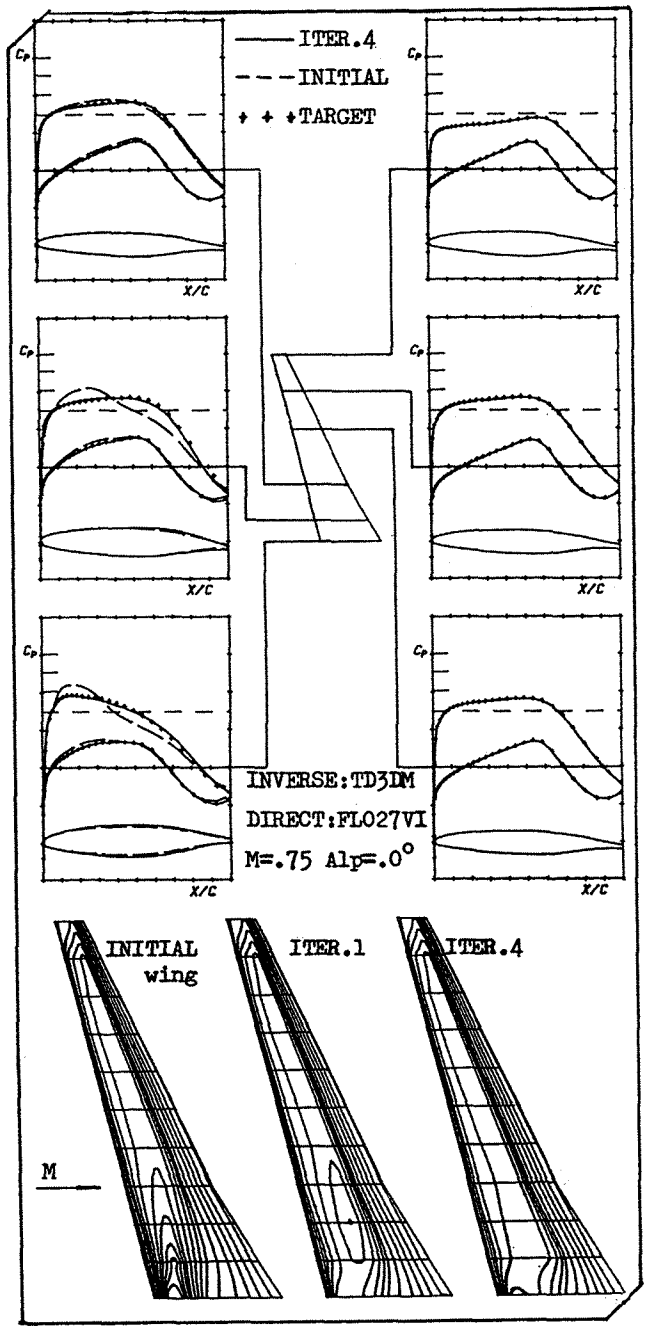

Fig. 9 Design result of a FSW

3.3.2 Design of FSW Wing-Body

When the body is present, similar behaviour of the inboard Cp as in the BSW case is recognized. The inboard Cp distribution is re-specified and the design is repeated with the body included in each of the direct mode. It takes another 10 iterations to get back to the Cp distributions as wing alone. Fig. 10 gives the comparison of isobars and Fig. 11 shows the difference of section contours. Unlike BSW, in this case both inboard sections become thicker.

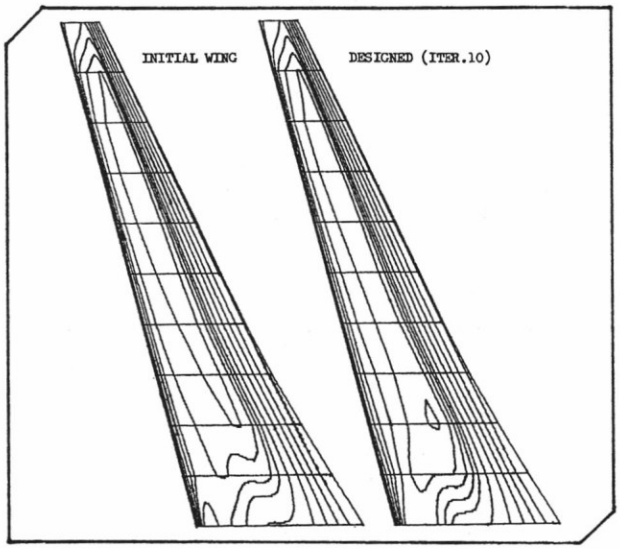

Fig. 10 Design result of FSW wing-body

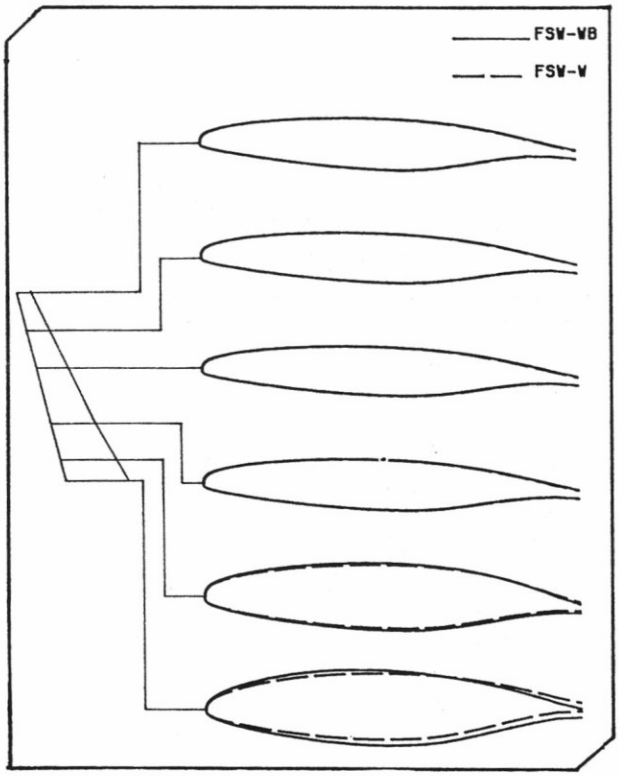

Fig. 11 Comparison of FSW control sections with and without body

4. Experimental Investigation

Experiment consists of the following measurements on low and high speed models of the NLF1 wing[29]:

a. wing surface pressure distributions;

b. transition locations;

c. wing aerodynamic characteristics; and

d. effect of changing wing sweep angles.

4.1 Experimental Setup

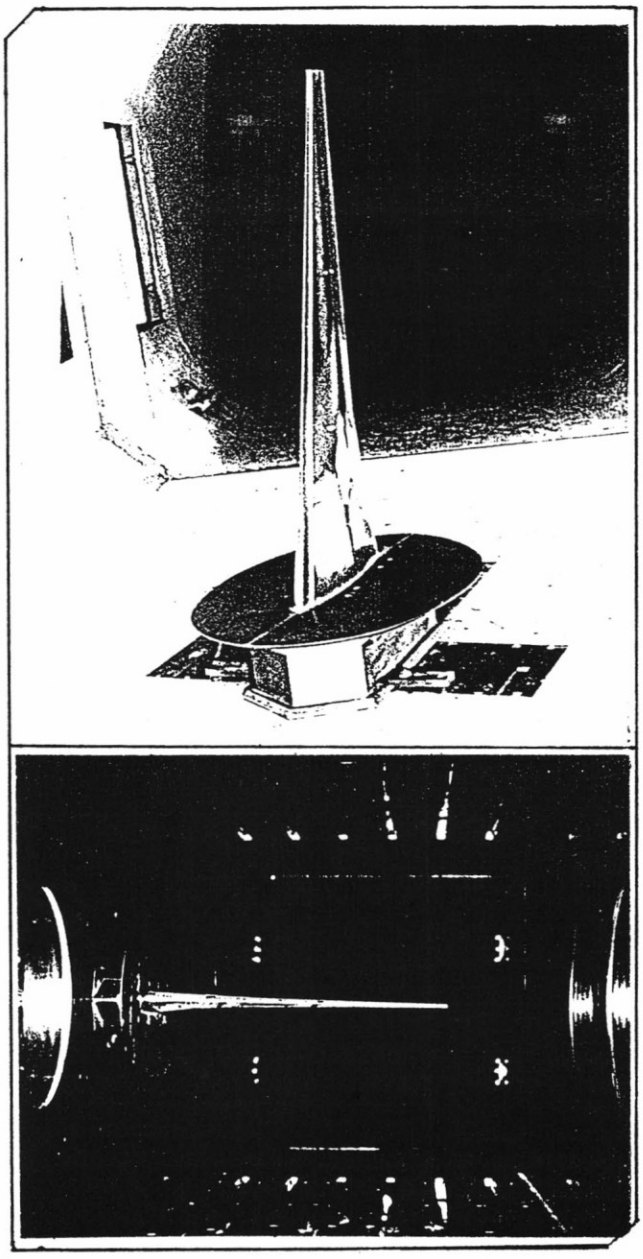

Fig. 12 Installation of the models upper: low-speed model in NH-2 lower: high-speed model in NH-1

4.1.1 Models

Half-wing models are designed for low and high speed tests, respectively. The low speed one is a 1:9 scale model of semi-span 1.4 m made of wood and metal, with 114 pressure orifices at $z=0.2$, 0.5 and 0.8 semi-span sections and 16 pieces of hot film at $z=0.3$ and 0.6 sections. The high speed model, 1:31 in scale, is made of metal with 54 orifices at $z=0.22$ and 0.55 semi-span stations. All the orifices are distributed in lines of 15° between the coming flow direction. Both models have the possibility to change the sweep angle.

4.1.2 Wind Tunnels

The low speed wind tunnel NH-2 has a test section of 3m x 2.5m, turbulent level 0.1%, test Re number of this wing model at $M=0.2$ is about 1.44 million.

The high speed tunnel NH-1 has a test section of 0.6m x 0.6m, speed region $M=0.5$ to $M=3.5$, test Re number of NLF1 high speed model is around 1.5 million.

Measuring instruments include HP1000-A700 computer, HP2250 sub-system, ESP and 780B pressure measuring system and a six-component strain gauge balance which is used in low speed tests.

Fig. 12 shows the installation of both models in wind tunnels.

4.2 Experimental Results

Selected results are given in the following figures:

Fig. 13 shows a comparison of Cp distributions between measurements and calculation (FLO22 mid.-mesh) near design condition. The agreement at upper surface is reasonable.

Fig. 14 and 15 are pictures of transition measurements from low and high speed tests, sublimate material and oil patterns are used, respectively. From both pictures, straight transition lines could be seen, suggesting that the isobar criterion has been realized, even at high speed case laminar seperation takes place. This is then checked with a 2D-analysis method at test Re number, similar seperation bubbles are indicated by the computation.

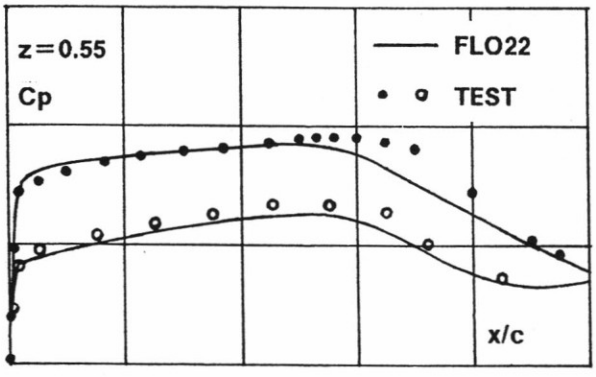

Fig. 13 Comparison of the calculated and measured Cp distributions $M=0.75,\alpha=0°$

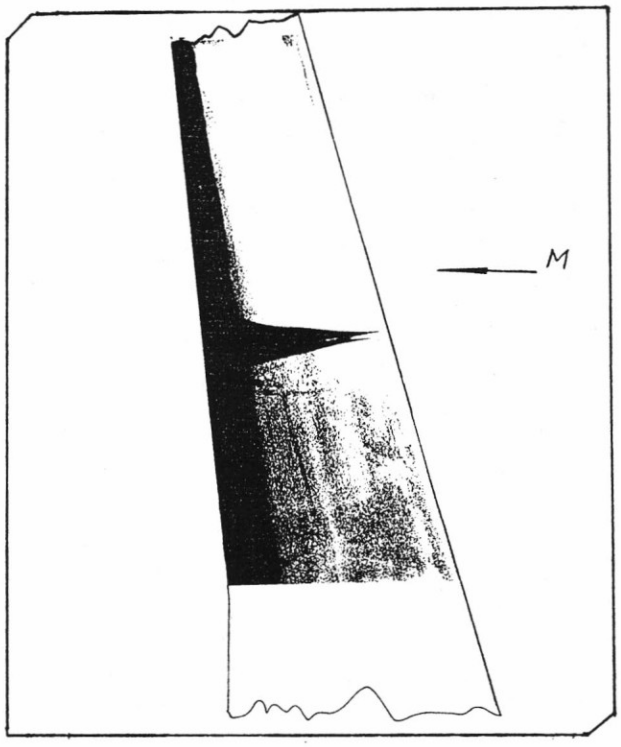

Fig. 14 Transition measured by Flow patterns, low-speed model, upper surface, $M=0.20,\alpha=0°$

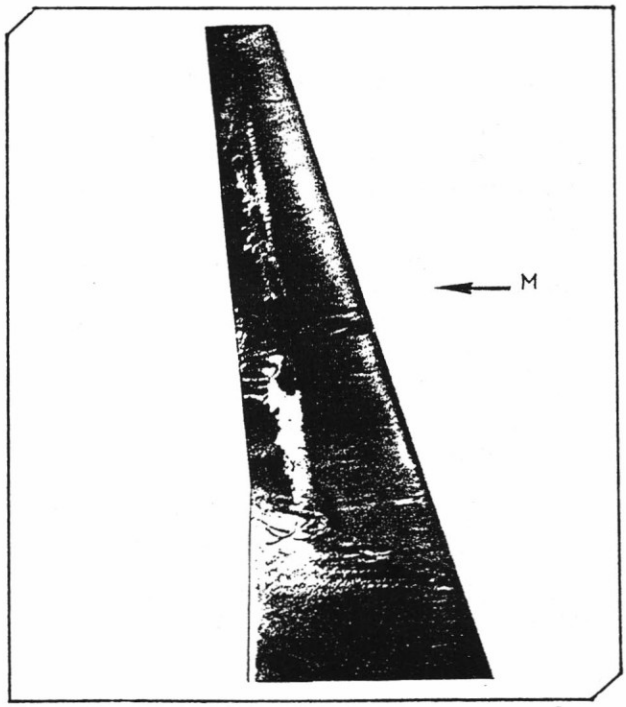

Fig. 15 Transition measured by oil patterns, high-speed model, upper surface, $M=0.75,\alpha=0°$

Fig. 16 gives the transition prediction by hot film method, which coincides well with the surface patterns.

Wing aerodynamic coefficients are measured from low speed test with free and fixed transitions. Great amount of drag recuction in the free transition case convinces of the advantage of NLF techniques.

The experiment also shows that reducing the leading edge sweep angle from 19° to 14° and 9° has little effect on the transition locations.

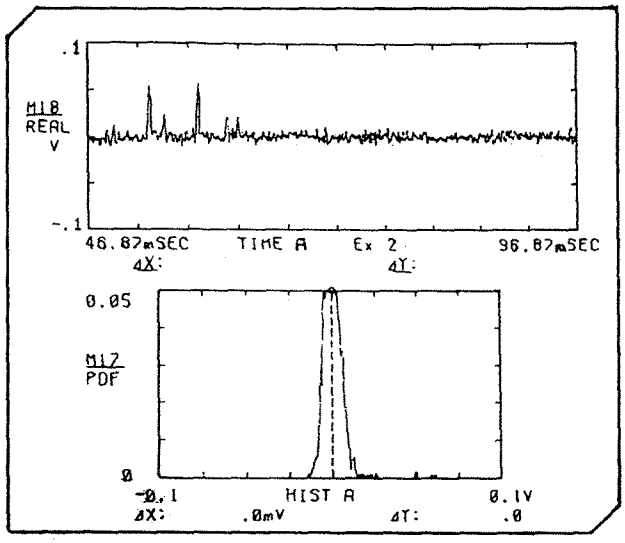

Fig. 16 Transition measured by hot films, low-speed model, upper surface, M=0.20,α = 0°, 70% chord

5. Conclusions

- In order to speed up the progress of Design Aerodynamics, more attention should be paid to the development of practical inverse methods.
- Design practice of NLF wings shows the necessity of including mixed boundary layer correction and other effects in the design methods.
- Design and experimental techniques are verified through the low and high speed wind tunnel tests.
- Numerical and Experimental investigations suggest that the present software, being successfully extended to NLF wing designs, could serve as an effective and practical design tool for transonic configurations.

6. Acknowledgement

This work is under a topic of Civil-Aircraft Pre-research Project of the Aviation Industries of China.

During the development of the theoretical methods and the 2D/3D- software, supports are also obtained from National Natural Science Foundation of China, Aeronautical Science Foundation, National Education Commitee Foundation and DLR-CAE cooperation projects.

References

[1] H. Körner: *Natural Laminar Flow Research for Subsonic Transport Aircraft in the FRG*. Lecture at ICAS'88, 1988

[2] G. Redeker, K.H. Horstmann, H. Köster: *Design of a Natural Laminar Flow Glove for a Transport Aircraft*. AIAA-90-3043-CP, 1990

[3] R.D. Wagner, M.C. Fische, F.S. Collier, W. Pfenninger: *Supersonic Laminar Flow Control on Commercial Transports*. ICAS-90-3.6.3, 1990

[4] E. Greff: *Aerodynamic Design of a New Regional Aircraft*. ICAS 90-2.7.1, 1990

[5] N. Hirose: *Numerical Wind Tunnel Project and Computational Fluid Dynamics at NAL, Japan*. 3rd ISNaS Symposium 1991

[6] K.H. Horstmann, G. Redeker, A. Quast, U. Dressler, H. Bieler: *Flight Tests with a Natural Laminar Flow Glove on a Transport Aircraft*. AIAA-90-3044-CP, 1990

[7] W. Nitsche, J. Szodruch: *Concepts and Results for Laminar Flow Research in Wind Tunnel and Flight Experiments*. ICAS-90-6.1.4, 1990

[8] R.L. Bengelink, P.E. Rubbert: *The Impact of CFD on the Airplane Design Process: Today and Tomorrow*. iPAC-911989, 1991

[9] L.A. Carlson: *Transonic Airfoil Analysis and Design Using Cartesian Coordinates*. J. Aircraft, Vol. 13, pp. 349-356, 1976

[10] G.B. McFadden: *An Artificial Viscosity Method for the Design of Supercritical Airfoils*. NASA-CR-158840, 1979

[11] P.A. Henne: *Inverse Transonic Wing Design Method*. J. Aircraft, Vol. 18, No. 2, 1981

[12] S. Takanashi: *An Iterative Procedure for Three-Dimensional Transonic Wing Design by the Integral Equation Method*. AIAA-84-2155, 1984

[13] M.B. Giles, M. Drela: *Two-Dimensional Transonic Aerodynamic Design Method*. AIAA J., Vol.25, No.9, 1987

[14] N. Hirose, S. Takanashi, N. Kawai: *Transonic Airfoil Design Based on Navier-Stokes Equations to Attain Arbitrarily Specified Pressure Distribution---an Iterative Procedure*. AIAA-85-1595

[15] J. Hua: *Design Research of Transonic Wings and Airfoils*. Ph.D. Thesis, NPU, 1989

[16] J. Hua, Z.Y. Zhang: *Transonic Wing Design for Transport Aircraft*. ICAS-90-3.7.4, 1990

[17] J. Hua, Z.Y. Zhang, Z.D. Qiao, P.S. Wang: *A Transonic Airfoil Design Method and Examples*. ACTA AERODYNAMICA SINICA, Vol.8, No.2, 1990

[18] J. Hua, Z.Y. Zhang, N.G. Shi, G. Redeker, H. Koster: *A Numerical Design Method for Modern NLF Airfoils*. ACTA AERODYNAMICA SINICA, Vol.11, No.1, 1993

[19] J. Hua, Q.Z. Yang, D.K. Xi, Z.Y. Zhang: *Numerical Design Methods for Transonic NLF Configurations*. JSASS 30th Aircraft Symposium, 1B5, 1992

[20] G. Wichmann, Z.Y. Zhang: *Calculation of Three Dimensional Transonic Wing Flow by Interaction of a Potential and an Integral Boundary Layer Method*. DFVLR IB 129-89/12, 1989

[21] R. Radespiel: *Erweiterung eines Profilberechungsverfahren im Hinblick auf Entwurfs- und Nachrechnungen von Laminarprofilen für Verkehrsflugzeuge*. DFVLR IB, 1981

[22] N. Kroll: *Solution of Two-Dimensional Euler Equations --- Experience with a Finite Volume Code*. DFVLR FB87-41, 1987

[23] J.Q. Bai: *Two-Dimensional Euler Equations with Viscous Correction and the Applications in Transonic Airfoil Design*. NPU Master Degree Thesis, 1994

[24] Q.Z. Yang, Z.Y. Zhang: *Mixed Boundary Layer Calculation for Transonic Wings*. International Conference on Fluid Mechanics and Theoretical Physics. 1992

[25] G. Redeker, H.K. Horstmann, H. Koester, A. Quast: *Investigations on High Reynolds Number Laminar Flow Airfoils*. ICAS 86-1.1.3, 1986. Also J. AIRCRAFT Vol. 25, No. 7, pp. 583-590, 1988

[26] G. Redeker, G. Wichmann: *Forward Sweep --- A Favourable Concept for a Laminar Flow Wing*. AIAA-88-4418, 1988

[27] Z.D. Qiao, W.H. Zhao, Y.B. Li, G.H. Bao: *The Transonic Wind Tunnel Test Research for the Supercritical Natural Laminar Airfoil NPU-L72513*. Aerodynamic Experiment and Measurement & Control, Vol. 7, No. 2, 1993

[28] D.B. Tang et. al. : *Investigation of Boundary Layer Stabilities and Transition for NLF Wings*. NUAA Report, MQ-02-01-88, 1990

[29] Z.L. Zhang, L. Wang, X.Z. Xiong, S.M. Zhang: *Experimental Verification of NLF1 Wing Models*. NUAA Report, MQ-02-04-88(0) 1990